Available online at www.sciencedirect.com
ScienceDirect
Journal of Solid State Chemistry 180 (2007) 1045–1050
JOURNAL OF SOLID STATE CHEMISTRY
www.elsevier.com/locate/jssc

Crystal structure, phase relations and electrochemical properties of monoclinic Li_2MnSiO_4

V.V. Politaev, A.A. Petrenko*, V.B. Nalbandyan, B.S. Medvedev, E.S. Shvetsova

Chemistry Faculty, Rostov State University, 7 ul. Zorge, Rostov-na-Donu 344090, Russia

Received 4 November 2006; received in revised form 20 December 2006; accepted 2 January 2007
Available online 13 January 2007

Abstract

Phase relations in the $MnO–SiO_2–Li_4SiO_4$ subsystem have been investigated by X-ray diffraction after solid-state reactions in hydrogen at 950–1150 °C. Both cation-deficient and cation-excess solid solutions $Li_{2+2x}Mn_{1-x}SiO_4$ ($-0.2 \leqslant x \leqslant 0.2$) based on Li_2MnSiO_4 have been found. According to Rietveld analysis, Li_2MnSiO_4 (monoclinic, $P2_1/n$, $a = 6.3368(1)$, $b = 10.9146(2)$, $c = 5.0730(1)$ Å, $\beta = 90.987(1)^\circ$) is isostructural with γ_{II}-Li_2ZnSiO_4 and low-temperature Li_2MgSiO_4. All components are in tetrahedral environment, $(MnSiO_4)^{2-}$ framework is built of four-, six- and eight-member rings of tetrahedra. Testing Li_2MnSiO_4 in an electrochemical cell showed that only 4% Li could be extracted between 3.5 and 5 V against Li metal. These results are discussed in comparison with those for recently reported orthorhombic layered Li_2MnSiO_4 and other tetrahedral Li_2MXO_4 phases.

Keywords: Lithium manganese silicium oxide; X-ray diffraction; Phase relations; Rietveld refinement; Solid solutions; Superstructure

1. Introduction

Li_2MnSiO_4 was briefly mentioned many years ago as an orthorhombic Li_3PO_4-type phase but its structure and even lattice parameters were not reported due to poor fit between observed and calculated d spacings [1]. We showed it to be monoclinic with angle β close but not equal to 90° [2]. Recently, this composition attracted attention ([3,4] and references therein) as a possible electrode material for lithium ion batteries. It was prepared at considerably lower temperature and exhibited a powder diffraction pattern entirely different from ours, with broad peaks and impurity phases; an orthorhombic cell was found by electron diffraction with edges similar to those of our monoclinic cell; a highly disordered tetrahedral structure was suggested with b parameter halved, but neither the space group nor R-factor was indicated [3].

We describe here crystal structure, phase relations and electrochemical properties of the monoclinic phase of Li_2MnSiO_4 and discuss the above discrepancies. Preliminary results on A_2MnXO_4 (A = Li, Na; X = Si, Ge) were reported elsewhere [5].

2. Experimental

Starting materials were reagent-grade Li_2CO_3, Mn_2O_3 and hydrous silica. Lithium carbonate was dried at 150 °C for two hours and two other reagents analysed for volatile components by measuring weight loss at 750 and 1000 °C, respectively. First of all, Li_2MnO_3 was prepared by solid-state reactions in air at 700–800 °C, and its phase purity was verified by X-ray diffraction (XRD). Then, it was mixed with calculated amounts of hydrous silica and, when necessary, Li_2CO_3 or Mn_2O_3, pressed and calcined in hydrogen atmosphere at various temperatures. It is well known that SiO_2 and MnO are stable to reduction with hydrogen whereas higher oxidation states of Mn are easily reduced. Thus, preparations in hydrogen atmosphere lead to ternary $Li_2O–MnO–SiO_2$ system rather than quaternary Li–Mn–Si–O.

XRD phase analysis was performed with a DRON-2.0 diffractometer in Ni-filtered Cu$K\alpha$ radiation. Higher-quality powder pattern used for the Rietveld structure

*Corresponding author. Fax: +7 863 297 5145.
E-mail address: apetrenko@rsu.ru (A.A. Petrenko).

0022-4596/$ - see front matter © 2007 Elsevier Inc. All rights reserved.
doi:10.1016/j.jssc.2007.01.001

refinement was recorded with a Geigerflex D/max-RC instrument with Cu$K\alpha$ radiation and secondary beam graphite monochromator. Corundum powder (NIST SRM 676) was used as an internal standard, assuming $a = 4.7592$ Å, $c = 12.9920$ Å. Refinement was performed using the GSAS + EXPGUI suite [6,7].

Sample for electrochemical testing was prepared from 87% Li_2MnSiO_4, 10% carbon black and 3% polytetrafluoroethylene as a binder dissolved in 1-methyl-2-pyrrolidone. The mixture was painted onto Al foil, dried at 70 °C for three hours and introduced, in a glove box filled with dry argon, into a three-electrode glass cell with electrolyte, 1 M $LiPF_6$ solution in diethyl carbonate + ethylene carbonate (1:1). Potentials were measured against a lithium reference electrode.

3. Results and discussion

3.1. Preparation and phase relations

Single-phase Li_2MnSiO_4 was prepared in two firings for two hours each at 700 and 1150 °C with intermediate regrinding and pressing. Its greyish white colour was characteristic of Mn (2+). The powder pattern was completely indexed using ITO program [8] on a monoclinic cell with lattice constants listed in Table 1. No impurity peaks could be detected at a sensitivity level of 0.2% of the strongest reflection. The Smith-Snyder figure of merit, $F(30) = 48$, characterizes these results as highly reliable.

Subsolidus phase analysis studies were complicated by slow kinetics, the relatively low melting point of lithium silicate eutectics, which delimited preparation temperatures, and also by difficulties with proper quenching. After heat treatment, the tube with samples and flowing hydrogen was cooled outside the furnace; still, this took several minutes. Thus, the results shown in Fig. 1 are only tentative and cannot be considered as strictly equilibrium and strictly isothermal data. The above difficulties are illustrated by the fact that different modifications of SiO_2 (quartz or tridymite) were observed after nominally identical heat treatments. $MnSiO_3$ in our samples was rhodonite.

Besides Li_2MnSiO_4, no new phases have been observed in the triangle MnO–SiO_2–Li_4SiO_4 (Fig. 1). However, extensive solid solutions exist along the orthosilicate join and, possibly, along the metasilicate join. For Li_2MnSiO_4, a bilateral homogeneity range has been found: $Li_{2+2x}Mn_{1-x}SiO_4$ ($-0.2 \leqslant x \leqslant 0.2$), suggesting both cation-deficient and cation-excess solid solutions. Possibly, high-temperature homogeneity range is even wider but partial dissolution occurs during relatively slow cooling. Compositional dependence of the lattice parameter **a** (Fig. 2) indicates a singularity for the stoichiometric composition, $x = 0$.

3.2. Crystal structure

Lattice constants and relative XRD intensities of Li_2MnSiO_4 are similar to those for γ_{II}-Li_2ZnSiO_4 [9]

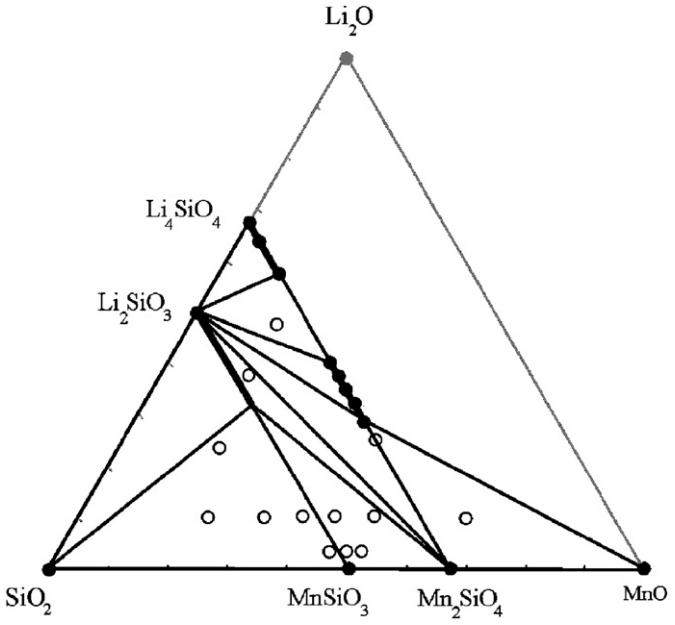

Fig. 1. Tentative subsolidus phase compatibility diagram for Li_2O–MnO–SiO_2 system at 950–1050 °C. Filled circles, single-phase samples; open circles, mixed-phase samples. The triangle adjacent to Li_2SiO_3–SiO_2 join could not be studied due to low melting temperatures.

Table 1
Crystallographic data for some tetrahedral Li_2MXO_4 structures

Phase	Space group	a (Å)	b (Å)	c (Å)	β (deg.)
γ_{II}-Li_2ZnSiO_4 [9]	$P2_1/n$	6.262(3)	10.602(4)	5.021(4)	90.51(5)
Low-temp. Li_2MgSiO_4 [10]	$P2_1/n$	6.300(0)	10.692(2)	4.995(5)	90.47(1)
Same [11]	$P2_1/n$	6.2889(5)	10.681(2)	4.9924(7)	90.46(1)
Li_2MnSiO_4 (this work) [2]	$P2_1/n$	6.3344(4)	10.9108(7)	5.0703(4)	90.990(9)
Li_2MnSiO_4 [3]	$Pmn2_1$ (?)	6.3109(9)	(2 ×) 5.3800(9)	4.9662(8)	
β_{II}-Li_2CoSiO_4 [12]	$Pbn2_1$	6.253(5)	10.685(9)	4.929(9)	
Li_2FeSiO_4 [13]	$Pmn2_1$	6.2661(5)	5.3295(5)	5.0148(4)	
Li_2CdGeO_4 [14]	$Pmn2_1$	6.64	5.47	5.130	
Li_2MnGeO_4 [5]	$Pmn2_1$	6.4653	5.4725	5.0501	
Li_2ZnGeO_4 [15]	Pn	6.400	5.45	5.04	90.2
Li_2CdSiO_4 [16]	$Pmnb$	6.479(1)	10.715(2)	5.119(1)	

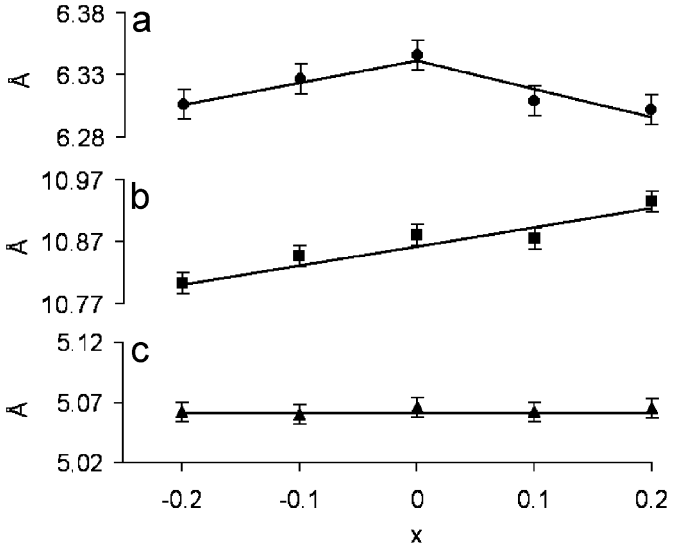

Fig. 2. Monoclinic lattice parameters of $Li_{2+2x}Mn_{1-x}SiO_4$ solid solutions. Error bars correspond to ± 2 standard deviations. Angle β (not shown) is approximately constant, 90.9(3)°, over the entire composition range.

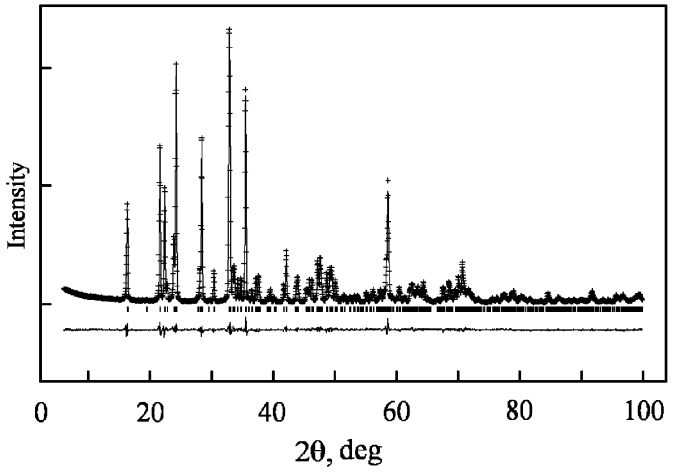

Fig. 3. Observed (crosses), calculated (solid line) and difference (bottom) XRD profiles of Li_2MnSiO_4. Vertical bars indicate Bragg positions.

(see Table 1). All observed reflections obey extinctions rules for space group $P2_1/n$. Thus, structure of Li_2ZnSiO_4 was taken as a reasonable starting model, with Mn on Zn site, and this model was successfully refined. Observed, calculated and difference XRD profiles are shown in Fig. 3. Refinement details and results are listed in Tables 2–4.

Since Li^+, Mg^{2+}, Zn^{2+} and Mn^{2+} have similar ionic radii, their mutual substitution seems quite possible. It is confirmed by the above phase analysis data and by single-crystal X-ray study of Li_2MgSiO_4 [11] revealing 2%, 20% and 78% Mg on three Li/Mg sites, respectively. On the other hand, no Li/Zn or Li/Mg substitution was indicated in the single-crystal XRD study of Li_2ZnSiO_4 [9] and powder neutron diffraction study of Li_2MgSiO_4 [10], although these two experiments might be, in principle, more sensitive due to much greater differences in scattering factors of the substituting and substituted ions. Small degree of substitution was merely not considered in these works.

Table 2
Crystallographic data, details of the X-ray powder data collection and Rietveld refinement of the Li_2MnSiO_4 structure

Crystal system	Monoclinic	2θ range	6–100 (deg.)
Space group	$P2_1/n$	Number of data points	4700
Lattice constants:			
a (Å)	6.336(1)	Number of reflections	773
b (Å)	10.9146(2)	Number of parameters	65
c (Å)	5.0730(1)		
β (°)	90.987(1)	Agreement factors	
Cell volume (Å^3)	350.8	R_p, %	4.64
Formula weight	160.90	R_{wp}, %	6.12
Z	4	χ^2	4.39

We refined Li/Mn ratio on each of the three sites. The total occupancy of each site was fixed to unity, negative occupancies forbidden, but total content of Mn was not restrained. Nevertheless, it was found to be $0.938+0.034=0.972$, i.e., very close to the nominal value of 1. This confirms the reliability of the result: a small but nonzero amount of Mn substitutes for Li and vice versa. The observed average bond lengths are in reasonable agreement with corresponding ionic radii sums (Table 4). Validity of the refined structure is further confirmed by the bond valence sums calculated by two different methods (Table 5).

Fig. 4 shows monoclinic structure of Li_2MnSiO_4 in comparison with idealized orthorhombic structure [3]. Both are based on slightly distorted hexagonal eutaxy (“close packing”) of oxygen ions with all “cations” in tetrahedral voids and pseudohexagonal plane parallel to (001), but differ in mode of filling the voids. Idealized orthorhombic phase is isostructural with the low-temperature Li_3PO_4, which, in turn, is a superlattice of wurtzite. All filled tetrahedra are in identical orientation along the **c**-axis (“all-up” [3]), and the structure is polar. On the other hand, monoclinic Li_2MnSiO_4 is a superlattice of the high-temperature orthorhombic Li_3PO_4, where equal amounts of tetrahedra are oriented in opposite directions along **c** making nonpolar structure and doubling **b**-axis. Mirror plane is eliminated by ordered arrangement of Li and Mn on sites, which were identical in the orthorhombic aristotype Li_3PO_4 structure, and this leads to slight monoclinic deformation.

The two structure types differ also in their mode of connecting tetrahedra (vertex-sharing only and partial edge-sharing, respectively) and in connectivity of their rigid part, $(MnSiO_4)^{2-}$. The orthorhombic phase is layered (2D) whereas the monoclinic phase is a framework (3D). The framework, however, is not of the cristobalite type as suggested earlier [2]. It is evident from Fig. 5, comparing the topology of linking tetrahedra in the five Li_2MXO_4 structure types listed in Table 1. Cristobalite-type framework with diamond-type topology is based exclusively on

Table 3
Atomic coordinates, occupancies and thermal parameters for Li_2MnSiO_4

	x	y	z	U_{iso} (Å^2)	Occupancy
Mn	0.5050(2)	0.1659(1)	0.3019(2)	0.00039(15)	0.938 Mn + 0.062 Li
Si	0.2538(3)	0.4137(2)	0.3123(4)	0.0082(3)	1
Li1	0.009(2)	0.1601(9)	0.300(2)	0.00025	1
Li2	0.2344(18)	0.0770(9)	0.7127(19)	0.046(4)	0.966 Li + 0.034 Mn
O1	0.2589(6)	0.4116(3)	0.6371(7)	0.063(4)	1
O2	0.2516(6)	0.5556(3)	0.1959(7)	0.00025	1
O3	0.0392(5)	0.3389(3)	0.2125(6)	0.00012(13)	1
O4	0.4647(7)	0.3435(3)	0.1981(7)	0.0064(13)	1

Table 4
Selected interatomic distances (Å) for Li_2MnSiO_4 and corresponding ionic radii sums [17]

Bond lengths							
Mn–O1	2.012	Si–O1	1.648	Li1–O2	1.896	Li2–O4	1.917
Mn–O2	2.023	Si–O3	1.654	Li1–O1	1.941	Li2–O1	1.960
Mn-O4	2.024	Si–O2	1.658	Li1–O3	2.011	Li2–O2	2.089
Mn–O3	2.091	Si–O4	1.658	Li1–O4	2.047	Li2–O3	2.138
Average sum of radii							
Mn–O	2.038	Si–O	1.655	Li1–O	1.974	Li2–O	2.026
Mn–O	2.04	Si–O	1.64	Li–O	1.97	Li–O	1.97

Table 5
Bond valences and their sums according to Brown and Altermatt [18] (**A**) and Pyatenko [19] (**B**)

A	O1	O2	O3	O4	ΣV
Li1	0.277	0.313	0.229	0.207	1.026
Li2	0.263	0.186	0.163	0.295	0.907
Mn	0.549	0.533	0.443	0.531	2.056
Si	0.977	0.953	0.963	0.953	3.846
ΣV	2.066	1.975	1.798	1.986	
B	O1	O2	O3	O4	ΣV
Li1	0.261	0.281	0.235	0.223	1
Li2	0.273	0.225	0.211	0.291	1
Mn	0.524	0.513	0.451	0.512	2
Si	1.024	0.987	1.002	0.987	4
ΣV	2.082	2.006	1.899	2.013	

six-member rings of tetrahedra (Fig. 5a), whereas monoclinic Li_2MSiO_4 (M = Mg, Mn, Zn) frameworks contain four-, six and eight-member rings (Fig. 5b). Li_2CoSiO_4 [12], although not isostructural with the above phases (see Table 1), surprisingly has the same topology. Two different layered structure types also have identical topology and contain exclusively four-member rings (Fig. 5c).

A further difference between the two Li_2MnSiO_4 polymorphs is that our phase, prepared at 1150 °C, is well crystallized and almost completely ordered, whereas the orthorhombic phase, prepared at low temperature of 700 °C, i.e., far from equilibrium, is highly disordered. Besides 10% Mn substitution for Li, each main Li, Mn and Si site has a neighbouring interstitial site with 8–35% occupancy at a distance of 0.5–1.1 Å in a face-shared tetrahedron [3]. Adjacent main and interstitial sites, of course, cannot be occupied simultaneously. It seems most probable that interstitial sites result from an intergrowth or a mixture of two structure types discussed above, derived from low- and high-temperature Li_3PO_4. This suggestion also explains doubling of the b-axis, indicated by electron diffraction but not found by XRD [3]. Possible monoclinic deformation may explain the reported poor fit between observed and calculated d values for several Li_2MSiO_4 compounds considered to be orthorhombic [1].

It is worth noting here that the reported structure of Li_2FeSiO_4 [13], although claimed to be of low Li_3PO_4 type, differs significantly in that Li tetrahedra are in an orientation opposite to those in low Li_3PO_4 and orthorhombic Li_2MnSiO_4 [3]. Each Si tetrahedron shares edges with two Li tetrahedra and this creates two very short, hardly possible, Si–Li distances of 2.5 Å, in addition to two Fe–Li distances of 2.7 Å. Thus, it seems that the reported Li position [13] is incorrect.

3.3. Electrochemical properties

It is well known that the characteristic, i.e., most stable, coordination of Mn (4+) is octahedral and that of Mn (3+) is distorted octahedral or square-pyramidal. We were able to find in literature only one example of unambiguously proven $Mn^{4+}O_4$ tetrahedron, $Bi_{12}MnO_{20}$ [20], and only two unambiguous examples of $Mn^{3+}O_4$ tetrahedra: $K_6Mn_2O_6$ [21] and Na_5MnO_4 [22], both being extremely unstable compounds. This is in contrast to high-spin Mn (2+), for which tetrahedral coordination is very frequent.

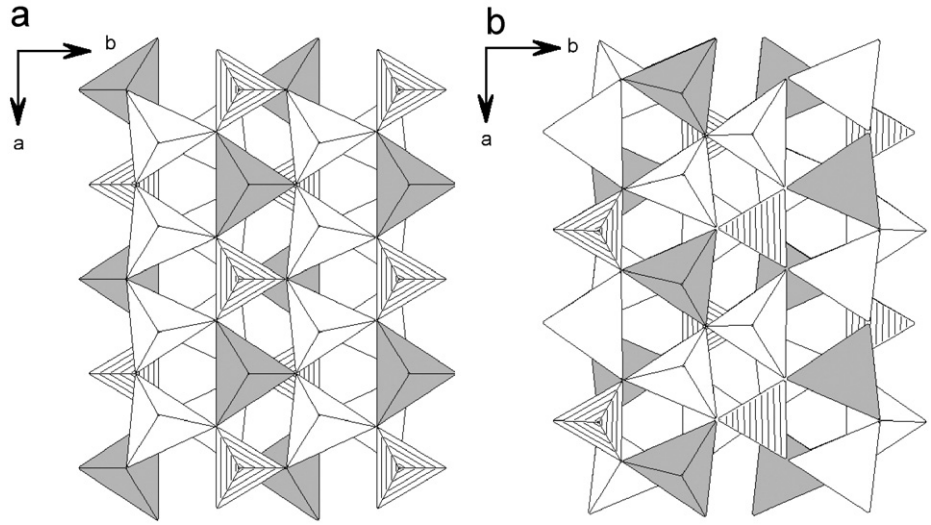

Fig. 4. Two crystal structures of Li_2MnSiO_4. Hatched tetrahedra, SiO_4; grey tetrahedra, MnO_4; white tetrahedra, LiO_4. (a) Orthorhombic structure [3], presumably $Pmn2_1$ (although not indicated explicitly), with only main positions shown (see text). (b) Monoclinic structure, $P2_1/n$ (this work).

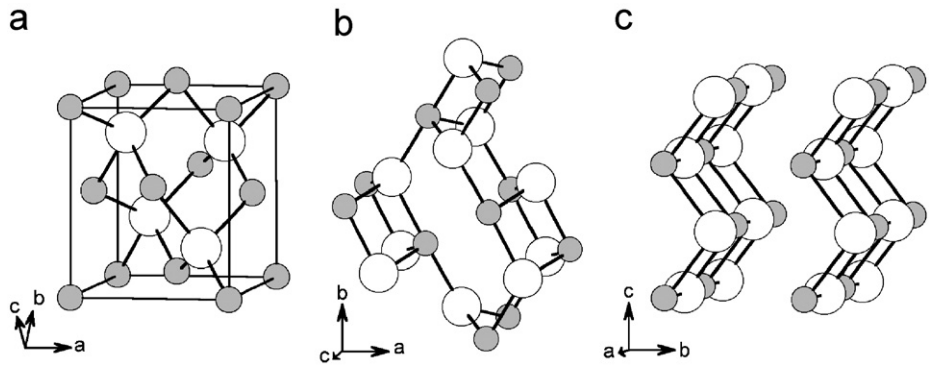

Fig. 5. Arrangement of divalent atoms M (large white balls) and tetravalent atoms X (small grey balls) in various Li_2MXO_4 structures. Bold lines connect atoms linked via common oxygen (not shown). (a) Li_2ZnGeO_4, Pn [15]. A sphalerite- or diamond-type pseudocell is shown by thin lines. (b) Li_2MSiO_4 (M = Mg [10,11], Zn [9], Mn), $P2_1/n$, and Li_2CoSiO_4, $Pbn2_1$ [12]. (c) Li_2CdSiO_4 [16], $Pmnb$, Li_2CdGeO_4 [14] and Li_2MnSiO_4 [3], $Pmn2_1$.

It is, thus, extremely difficult to oxidize Mn (2+) in situ, maintaining tetrahedral coordination; and, if this is still possible, the resulting tetrahedral Mn (3+) or Mn (4+) is expected to be a very strong oxidizer, providing high discharge voltage, favourable for practical use.

The open-circuit voltage (OCV) of our Li_2MnSiO_4-based electrode is 3.52 V against lithium. Coupled with high theoretical charge capacity of 333 mA h/g (calculated for extraction of two lithium ions) this seems very attractive. However, charging experiments show very strong polarization even at low current density of 0.05 mA/cm^2 (0.015 C rate). On passing of only 4% of the above charge, voltage grows to 5 V making further charging impossible. After 12 h, the OCV of the charged cell stabilizes at 3.76 V. On discharge, the voltage drops rapidly below 1.7 V.

This behaviour is in contrast with that of previously reported orthorhombic form [3]. It also exhibits irreversible behaviour but permits extraction of 50% Li between 3.3 and 4.5 V at the first cycle. This difference may be explained by

(i) Layered structure of the orthorhombic phase which provides more freedom for Li^+ ion motion and, possibly, for Mn displacement into octahedral voids (unfortunately, XRD data of the charged electrode are not available);
(ii) Considerably smaller particle size of the material prepared at 700 °C (compared to our 1150 °C);
(iii) Presence of conductive impurity, a carbon resulting from decomposition of organic precursors [3], providing better electrical contacts than our mechanical mixing with mortar and pestle.

In any case, both data sets show that neither form of Li_2MnSiO_4 is suitable for practical use in rechargeable lithium ion batteries.

4. Conclusions

X-ray phase analysis study of the $MnO–SiO_2–Li_4SiO_4$ subsystem revealed formation of only one ternary compound having a bilateral homogeneity range $Li_{2+2x}Mn_{1-x}SiO_4$ ($-0.2 \leqslant x \leqslant 0.2$). According to Rietveld analysis, Li_2MnSiO_4 is monoclinic, isostructural with γ_{II}-Li_2ZnSiO_4 and low-temperature Li_2MgSiO_4. A comparison of this structure with orthorhombic Li_2MnSiO_4 [3] shows that both are based on hexagonal close packing of oxygen ions with all components having tetrahedral environment but differ in topology of their rigid part, $(MnSiO_4)^{2-}$: the monoclinic modification is a framework whereas the orthorhombic phase is a layered structure. This, together with the smaller particle size of the orthorhombic phase and presence of a conducting impurity (carbon), explains its better charging behaviour in a lithium ion cell. However, neither modification is suitable for battery applications.

Acknowledgments

The work was supported by the International Centre for Diffraction Data and Russian Federal program "Integration". The authors thank Dr. S.N. Polyakov for the Geigerflex scans.

References

[1] P. Tarte, R. Cahay, C.R. Acad. Sci. Paris C 271 (1970) 777–779.
[2] Powder Diffraction File, International Centre for Diffraction Data, 2005, 00-055-0704.
[3] R. Dominko, M. Bele, M. Gaberšček, A. Meden, M. Remškar, J. Jamnik, Electrochem. Commun. 8 (2006) 217–222.
[4] M.E. Arroyo-de Dompablo, M. Armand, J.M. Tarascon, U. Amador, Electrochem. Commun. 8 (2006) 1292–1298.
[5] V.V. Politaev, A.A. Petrenko, V.B. Nalbandyan, E.S. Shvetsova, IV National Crystal Chemistry Conference, Book of Abstracts, Chernogolovka, Russia, 26–30 June 2006, pp. 235–236. 〈http://www.icp.ac.ru/conferences/new/NCCC2006/thfiles/3/060202-0226979-Petrenko.rtf〉.
[6] A.C. Larson, R.B. VonDreele, General Structure Analysis System (GSAS), Los Alamos National Laboratory Report LAUR 86-748, 2004.
[7] B.H. Toby, J. Appl. Cryst. 34 (2001) 210.
[8] J.W. Visser, J. Appl. Cryst. 2 (1969) 89.
[9] H. Yamaguchi, K. Akatsuka, M. Setoguchi, Acta Cryst. B 35 (1979) 2678–2680.
[10] C. Jousseaume, A. Kahn-Harari, D. Vivien, J. Derouet, F. Ribot, F. Villain, J. Mater. Chem. 12 (2002) 1525–1529.
[11] L.D. Iskhakova, V.B. Rybakov, Crystallogr. Rep. 48 (2003) 39.
[12] H. Yamaguchi, K. Akatsuka, M. Setoguchi, Y. Takaki, Acta Cryst. B 35 (1979) 2680–2682.
[13] A. Nytén, A. Abouimrane, M. Armand, T. Gustafsson, J.O. Thomas, Electrochem. Commun. 7 (2005) 156–160.
[14] N.S. Korjakina, N.V. Suvorova, L.N. Dem'yanets, B.A. Maksimov, V.V. Ilyukhin, N.V. Belov, Dokl. Akad. Nauk SSSR 200 (1971) 329–332.
[15] E. Plattner, H. Voellenkle, A. Wittman, Monat. Chem. 107 (1976) 921–927.
[16] C. Riekel, Acta Cryst. B 33 (1977) 2656–2657.
[17] R.D. Shannon, Acta Cryst. A 32 (1976) 751–767.
[18] I.D. Brown, D. Altermatt, Acta Cryst. B 41 (1985) 244–247.
[19] Yu.A. Pyatenko, Kristallografiya 17 (1972) 773–779.
[20] U. Delicat, S.F. Radaev, M. Troemel, P. Behrens, Y.F. Kargin, A.A. Marin, J. Solid State Chem. 110 (1994) 66–69.
[21] G. Brachtel, R. Hoppe, Z. Anorg. Allgem. Chem. 446 (1978) 64–76.
[22] G. Brachtel, N. Bukovec, R. Hoppe, Z. Anorg. Allgem. Chem. 515 (1984) 101–113.